

Proceedings of the Fourth International Symposium  
on  
ADVANCED NUCLEAR ENERGY RESEARCH  
ROLES AND DIRECTION OF MATERIAL SCIENCE  
IN NUCLEAR TECHNOLOGY -

POSITRON ANNIHILATION STUDY OF GRAPHITE, GLASSY CARBON AND C<sub>60</sub>/C<sub>70</sub> FULLERENE

Masayuki Hasegawa, Masahiro Kajino, Tadao Iwata\*  
Eiichi Kuramoto\*\*, Minoru Takenaka\*\* and Sadae Yamaguchi

Institute for Materials Research, Tohoku University, Sendai 980, Japan  
Phone 022-227-6200 ext.2454, Fax 022-215-2061

\* Physics Department, Japan Atomic Energy Research Institute,  
Tokai, Ibaraki 319-11, Japan  
Phone 0292-82-5470, Fax 0292-82-5297

\*\* Research Institute for Applied Mechanics, Kyusyu University,  
Kasuga, Fukuoka 816, Japan  
Phone 092-573-9611 ext. 566, Fax 092-582-4201

**ABSTRACT:** ACAR ( Angular Correlation of Annihilation Radiation) and positron lifetime measurements have been made on, HOPG (Highly Oriented Pyrolytic Graphite), isotropic fine-grained graphite, glassy carbons and C<sub>60</sub>/C<sub>70</sub> powder. HOPG showed marked bimodality along the c-axis and anisotropy in ACAR momentum distribution, which stem from characteristic annihilation between "interlayer" positrons and  $\pi$ -electrons in graphite. ACAR curves of the isotropic graphite and glassy carbons are even narrower than that of HOPG perpendicular to the c-axis. Positron lifetimes of 420 and 390 - 480 psec, much longer than that of 221 psec in HOPG, were observed for the isotropic graphite and glassy carbons respectively, which are due to positron trapping in structural voids in them. Positron lifetime and ACAR width (FWHM) can be well correlated to void sizes (1.7 to 5.0 nm) of glassy carbons which have been determined by small angle neutron (SAN) scattering measurements. ACAR curves and positron lifetime of C<sub>60</sub>/C<sub>70</sub> powder agree well with those of glassy carbons. This shows that positron wave functions extend, as in the voids of glassy carbons, much wider than open spaces of the octahedral interstices of the face-centered cubic (FCC) structure of C<sub>60</sub> crystal and strongly suggests positron trapping in the "soccer ball" vacancy. Possible positron states in the carbon materials are discussed with a simple model of void volume-trapping. Preliminary results on neutron irradiation damage in HOPG are also presented.

---

**Keywords:** Positron Annihilation, Graphite, Glassy Carbon, C<sub>60</sub>, Fullerene, Void, Pore, Void Trapping, Soccer Ball Vacancy

---

## 1. INTRODUCTION

Graphite has been employed as the moderator and structural components of fission reactors, such as gas-cooled one, because of low neutron cross section, chemical stability and high melting point. Further recently carbon materials, for example graphite and carbon-carbon composites, have become one of the key materials in the field of plasma-wall interaction in fusion reactors because of its low atomic number and high-temperature characteristics. For fusion reactor application, absorption and desorption of hydrogen isotope atoms are very important and sensitively affected by structural voids\*) and radiation-induced vacancies and voids. Consequently atomistic information and characterization of structural voids and radiation-induced defects is very necessary. Positron annihilation has been successively used for studies of vacancies and voids in metals [1]. For carbon materials the usefulness of this technique has been demonstrated by several workers [2-6].

---

\*) sometimes called as cavities or pores.

Recent exciting report of method for preparing large quantities of the "soccer ball"  $C_{60}$  molecules [7] and the following discovery of superconductivity in potassium-doped  $C_{60}$  [8] have raised great interest in the structure and properties of this allotropic form of carbon [9,10]. Because of the weak intermolecular interaction, the solid  $C_{60}$  has large open spaces, for example, at the octahedral interstices where potassium atoms can be accommodated in its structure. Consequently it is very interesting to investigate positron states in solid  $C_{60}$  and to compare them with those in graphite and glassy ( glass-like ) carbon.

Recently positron lifetime measurements have been carried out by several groups [11-13], including us [6]. Further theoretical calculations show positron states and lifetimes in  $C_{60}$  and potassium-doped fullerenes [14,15]. All these experimental studies have reported a positron lifetime of about 400 psec in  $C_{60}$  powders. This value is in good agreement with calculated one from theoretical model in which positron wave function is highly concentrated in an octahedral interstices of the FCC structure. The lifetime of 400 psec is much longer than that in graphite bulk ( about 220psec ) or vacancy (about 245 psec [4]), but very close to that observed in glassy carbon and irradiated graphite[3-6]. Then it is very necessary to make systematic study on carbon materials, such as  $C_{60}$ , graphite and glassy carbons. In this paper results of ACAR and positron lifetime measure

ments on HOPG, glassy carbons and  $C_{60}/C_{70}$  powder will be compared and discussed with a simple void-trapping model.

## 2. EXPERIMENTAL

Figure 1 shows crystal structures of diamond (a), graphite (b) and the (100) face of the FCC  $C_{60}$ . Samples used in this study are listed in Tab.1. A single crystal plate of synthetic diamond with (111) crystal face was used. Highly oriented pyrolytic graphite (HOPG) (ZYA and ZYH grade, Union Carbide Co.) slabs have mosaic structure with the well-oriented c-axis but with random orientation of the crystallites in the basal plane. The average crystallite size along the a-axis is about  $25\mu\text{m}$  while  $7\mu\text{m}$  along the c-axis [3]. HOPG-ZYA was subjected to fast neutron irradiation with fluence of  $8.3 \times 10^{18} \text{ n/cm}^2$  at about  $150^\circ\text{C}$  in the JMTR reactor. The block of HOPG-ZYH was irradiated to  $1.4 \times 10^{20} \text{ n/cm}^2$  at about  $60^\circ\text{C}$  in the JRR-2 reactor. Isotropic fine-grained nuclear graphite, AXF-5Q1 (POCO Graphite Inc.), graphitized at  $2500^\circ\text{C}$ , has an average grain size of about  $4\mu\text{m}$  and void radii ranging from 0 to  $0.4\mu\text{m}$ . The grains consist of crystallites ( about  $40\text{nm}$  both along the a-axis and c-axis [8] ) plus voids among them as schematically shown in Fig. 1 (e)[16]. Glassy carbon is a kind of non-graphitizable hard carbons [17] and has a microstructure in which voids are surrounded by carbon layers of graphite or turbostratic stacking with thickness less than about 10 layers as depicted in Fig.1(d) [19].

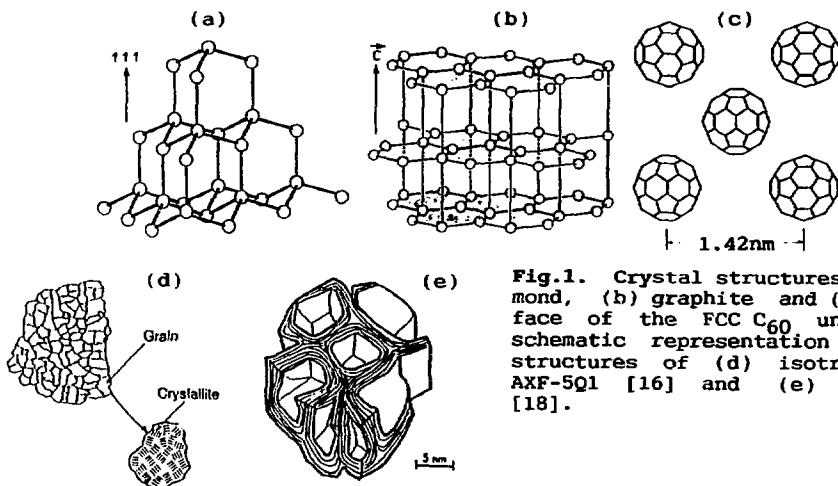


Fig.1. Crystal structures of (a) diamond, (b) graphite and (c) the (100) face of the FCC  $C_{60}$  unit cell, and schematic representation of the microstructures of (d) isotropic graphite AXF-5Q1 [16] and (e) glassy carbon [18].

Table 1. Specimens, their densities, ACAR FWHM widths and positron lifetimes.

Specimen	Density (g/cm <sup>3</sup> )	ACAR FWHM (mrad)	Lifetime (psec)	Remarks
Diamond	3.51	13.1	107.1	
HOPG	2.26			
Unirrad. (ZYA)		$c_{//}$ : 13.4 $c_{\perp}$ : 10.9	221.0	$c = 0.670$ nm $a = 0.246$ nm
Irrad. (ZYA)		$c_{//}$ : 11.4 $c_{\perp}$ : 10.2	283.1	$8.3 \times 10^{18}$ n/cm <sup>2</sup>
Irrad. (ZYH)		$c_{//}$ : 9.1 $c_{\perp}$ : 8.5	363.9 (96%)	$1.4 \times 10^{20}$ n/cm <sup>2</sup> $\Delta c/c = 10.2\%$ $\Delta a/a = -0.7\%$
Isotropic Graphite AXF-5Q1	1.84	10.3	381.0	
Glassy Carbon GC-10	1.49	10.3	392.5	Rg = 0.65 nm
GC-20	1.48	9.5	480.7	Rg = 1.29 nm
GC-30	1.45	9.3	466.0	Rg = 1.93 nm
C <sub>60</sub> /C <sub>70</sub>	1.7*)	9.4	416.7(300K) 405.6(10K)	

\*) theoretical density

Glassy carbons with different heat treatment temperatures (HTT) from TOKAI CARBON Co. were examined: GC-10, GC-20 and GC-20 heat-treated at 1300°C, 2000°C and 3000°C respectively. Small angle neutron scattering measurements have revealed that these samples contain voids of nearly uniform size with radii of gyration (Rg) given in Tab.1 [19]. For fullerene sample, powder of C<sub>60</sub>/C<sub>70</sub> (C<sub>60</sub> : 90%) of 98% purity (MER Co.) were employed.

Long-slit ACAR measurements were performed with a usual machine having a geometrical resolution of 0.63 mrad (FWHM) and <sup>64</sup>Cu sources of 1 Ci strength. Lifetime measurements were accomplished using a conventional apparatus with a time resolution of about 170 psec (FWHM), much higher resolution than that of the preceding paper [6], and <sup>22</sup>Na (20 μCi) source deposited on to a thin mylar film. Measurements are carried out at room temperature otherwise stated. After source-background subtraction, lifetime spectra were decomposed into one or two lifetime component using a fitting program.

### 3. RESULTS AND DISCUSSION

#### 3-1 Diamond and Graphite

Figure 2 shows ACAR curves of diamond, unirradiated HOPG-ZYA samples for  $p_z$ , momentum examined, (a) parallel to the c-axis [PZPC] and (b) normal to the c-axis [PZNC] as well as AXF-5Q1. Although statistics for diamond is poor because of its very small size, the ACAR curve is clearly found to be very broad, which is due to small lattice constant and hence large Brillouin zone. As listed in Tab.1 positron lifetime in diamond is very short, being compare with typical semiconductors such as Si. This is also due to high density of the valence electrons in diamond. ACAR curves of HOPG-ZYH are in good agreement with those of HOPG-ZYA and then not shown here. For the unirradiated state the PZPC distribution is bimodal with a saddle point at  $p_z=0$  and peaks around  $p_z = \pm 3$  mrad, whereas bell-shaped for PZNC. The bimodal distribution is due to highly concentrated wave function of positron within a graphite layer (inter-layer positron) and its consequently enhanced annihilation with  $\pi$ -electrons

whose wave functions are extending along the c-axis with nodal planes of the graphite hexagonal network planes [20-23]. The salient bimodal distribution observed shows that almost all positrons have annihilated from delocalized Bloch state.

Irradiation of  $8.3 \times 10^{18}$  n/cm<sup>2</sup> on HOPG-ZYA caused disappearance of the bimodal shape and marked narrowing in the PZPC distribution (Fig.3). This is due to trapping of positrons in defects: vacancies - vacant sites at the network planes, where the positrons do not see  $\pi$ -electrons [4] - or microvoids as stated below. It should be noted that depth of the saddle point from the bimodal peak is very sensitive to presence of vacancy-type defects. In the PZNC distribution, narrowing by irradiation was observed to nearly the same extent as in usual metals, which also suggests positron trapping at the vacancy-type defects. Higher dose irradiation on HOPG-ZYH has induced further narrowing in the ACAR curves for both orientation. This implies that higher dose results in positron-trapping in larger vacancy-type defects. As a measure of gross shape of ACAR curve, FWHM width of the ACAR curves are presented in Tab.1, where for HOPG a full width at a half

height of the saddle point, instead of the peaks at 3 mrad, is given.

Lifetime spectra of unirradiated HOPG (ZYA and ZYH) were well represented by single lifetime of 221 psec (Tab.1). The results are consistent with previous work [4,5]. The lower dose irradiation (HOPG-ZYA) caused an increase in lifetime to 284 psec. Shimotomai et al. have reported that the lifetime of positrons trapped at vacancies is about 245 psec [4]. This indicates the lifetime of the irradiated HOPG-ZYA is an average between lifetimes coming from positron trapping at vacancies and very small microvoids, because of finite time resolution. The higher dose irradiation (HOPG-ZYH) gave a longer lifetime component of 364 psec ( Tab.1 ) and a short component of about 250 psec with very small intensity of about 4%, which is very close to positron lifetime in vacancy as stated above. The longer lifetime is due to radiation-induced microvoids as stated below.

Lifetime spectra of AXF-5Q1 is well decomposed to a single component of 381 psec, much longer the vacancy lifetime. ACAR curve and its FWHM width for AXF-5Q1 are shown in Fig.3 and Tab.1 respectively. The FWHM width is less

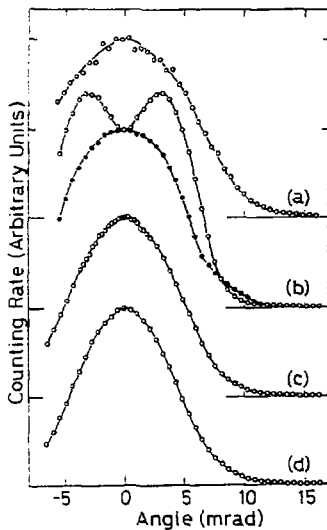


Fig.2. ACAR curves of (a) diamond, (b) HOPG, PZPC (○) and PZNC (●), (c) AXF-5Q1, and (d) C<sub>60</sub>/C<sub>70</sub> powder. All the curves are normalized to the same height at zero angle.

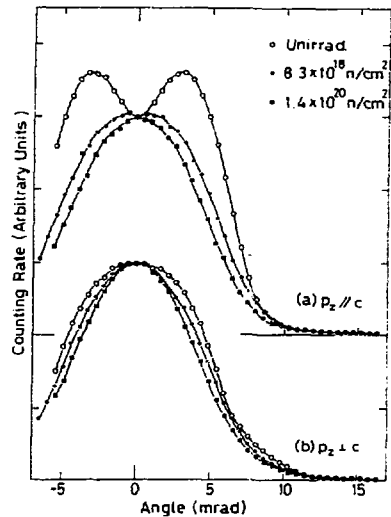


Fig.3. ACAR curves of the unirradiated and irradiated HOPG for (a) PZPC and (b) PZNC orientations.

than either of PZPC or PZNC orientation of the unirradiated HOPG. These results are possible only if most of positrons annihilate from trapped states of structural voids but not from delocalized state in the isotropic graphite: annihilation from delocalized state would give an intermediate width between those for the PZPC and PZNC orientations and rather flat shape around zero angle. It should be noted that vacancies or their very small microvoids can not exist because the sample has been heat-treated at high temperature of 2500°C.

We consider possible positron trapping in the structural voids. Artificial graphites are characterized by a significant (closed and opened) porosity among grains and voidage within grains (Fig. 1(d)). AXF-5Q1 is a fine-grained isotropic graphite which are extremely isotropic and of very small and uniform crystallite size [16]. Positrons in graphite bulk are well characterized as "interlayer positrons" between the hexagonal network planes and may have marked anisotropy in positron diffusion. However to our knowledge no experimental information on the diffusion has been reported. Then we simply assume positron diffusion constant of perfect graphite crystals  $D = 1 \text{ cm}^2/\text{sec}$ , as seen in metals and semiconductors [24], and get a diffusion length  $(D)^{1/2} = 200\text{nm}$  which is much longer than the crystallite size of 40nm. This suggests that most of positrons in the crystallite diffuse to the inter-crystallite voids, get trapped there and give the longer lifetime component and a narrow ACAR curve. Delocalized positron states in these void are discussed later.

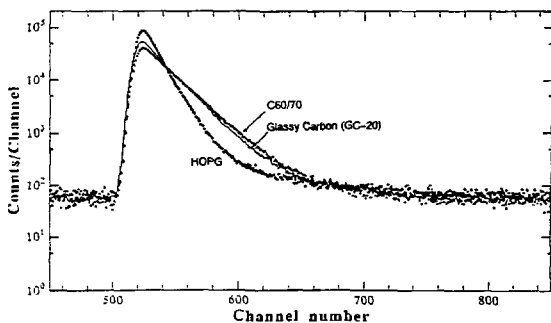


Fig.4. Positron lifetime spectra of HOPG, glassy carbon (GC-20) and  $C_{60}/C_{70}$  powder. Time scale is 23.2 psec/channel.

### 3-2 Glassy Carbons

ACAR curves of the glassy carbons, especially of GC-10, were found to be very similar to that of AXF-5Q1, as seen from their FWHM (Tab.1). ACAR curves of GC-20 (shown later in a comparison with  $C_{60}/C_{70}$  of Fig.5) and GC-30 are broader than that of GC-10. Lifetime spectra of the glassy carbons, for example GC-20 as presented in Fig.4, are well decomposed to single lifetime components of 390 - 480 psec (Tab.1). These results indicate that positrons in the glassy carbons are trapped in structural voids, as in the isotropic graphite. For samples of higher heat-treatment temperature (GC-20 and GC-30), narrowing in ACAR curve and increase in positron lifetime are observed (Tab.1). These changes by heat treatment are presumably due to growth of the voids, as seen in increase of  $R_g$  (Tab.1)[10]. Voids in glassy carbons are well known to have nearly spherical polyhedra bounded by graphite layer planes (Fig.1(e)) and to be uniform in size as revealed by Guinier plot of small angle scattering intensity (X-ray [25] and neutron [19]) and give well definite value of  $R_g$  as listed in Tab.1.

Natural question is about trapping state of positrons in the voids in the isotropic graphites and glassy carbons. Various void-trapping states in metals have been reported so far: void-surface of many metals [1], free positronium (Ps) in voids in V and Nb [26] and Ps-like state at void surface of Al [27]. For metals it is well known that ACAR FWHM width decreases and lifetime increases with the radius up to about 0.5

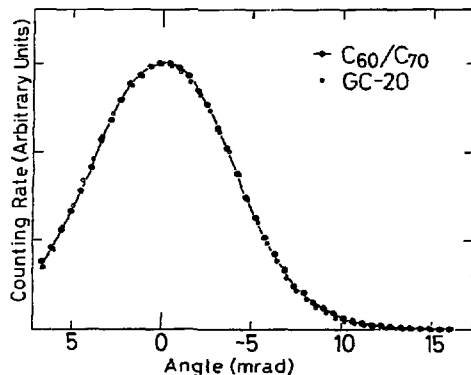


Fig.5. ACAR curves of  $C_{60}/C_{70}$  powder and GC-20.

nm. However, further increase in the radius does not give any change in ACAR curve and lifetime any more, which is interpreted as appearance of positron-trapping at the void surface (Fig.6(a)). The trapping state at the void surface has essentially the same physical origins as that at free surface: positrons are repelled toward vacuum by surface dipole potential induced spilled-out electrons while attracted by image force. Are they possible in carbon materials? On the contrary to the case of conduction electrons in metals, valence electrons in graphite cannot spill out from surface because of covalent bonding. Further formation of the

image potential could be supposed to be very limited if we notice that the electron pile-up to form the image potential is only done by  $\pi$ -electrons which can freely move along graphite hexagonal network plane, but not perpendicular to it.

Sferlazzo et al. [28], from slow positron experiment, have demonstrated that surface two dimensional (2D) ACAR spectrum is very similar to that of the bulk in HOPG, in contrast to the case of metal where the surface spectrum is substantially different from the bulk one. To explain the similarity they have proposed two possibilities: (1) the surface trapping state does not exist and the positron annihilate in the last few graphite layers (2) the electrons sampled by the surface-bound positrons are very similar to those sampled by the interlayer positrons in the bulk. We have to note here that formation of a surface-bound state for positron should be accompanied by significant change in the surface-electron states, especially of  $\pi$ -electrons, which will be detected in the 2D ACAR spectrum as stated above. Then we support the first possibility, no surface-trapping state of positrons. This is further supported by the results of AXF-5Q1 which is definitely characterized as small crystallites of nearly perfect graphite crystals plus voids among the crystallites and inter-granular voids. If the surface-trapping is possible in graphite and ACAR momentum distribution is nearly the same as that in the bulk, almost all positrons should be trapped at the void surface and give ACAR curve corresponding to an intermediate between the c-axis parallel [PZPC] and perpendicular [PZNC] ACAR curves. This is not consistent with the present result: the curve for AXF-5Q1 is narrower than even that for PZNC. Then we have to seek a possible alternative model of void trapping.

In HOPG the positron state are well explained in terms of a two dimensional state of delocalized interlayer positron sampling preferentially the  $\pi$ -electrons [22,29], as schematically depicted in Fig.6(b) with a separation of  $d = c/2$  between the hexagonal graphite layers. It should be noted that the positrons exist mostly in the interlayer region but hardly upon the graphite layer. Voids in glassy carbon are bounded by graphite layer planes ( as shown in Fig.1(e) ), sometimes accompanied with turbostratic stacking. Then we propose a

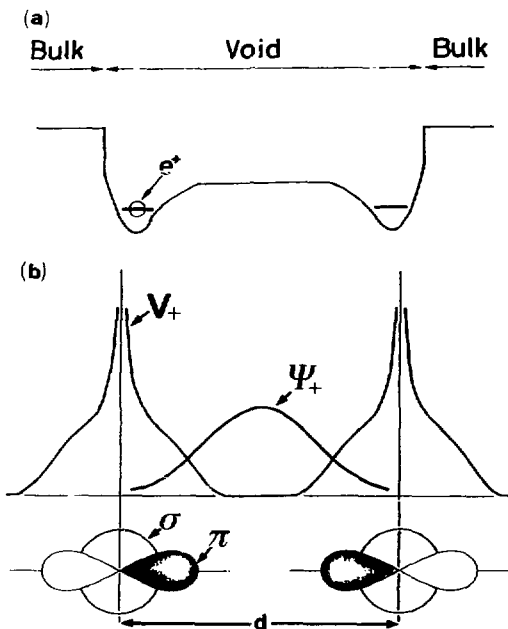


Fig.6. Schematic representation of possible positron trapping states in voids of graphite and glassy carbon, (a) surface trapping and (b) volume trapping. In (b) the vertical lines show facing hexagonal graphite-layers, with effective separation of  $d$  ( diameter), at the void surface. The limit of  $d = c/2$  could be assumed to correspond to interlayer positrons in the bulk of graphite. Schematics of effective potential energy ( $V_+$ ) of a positron near the graphite layer and of positron wave function ( $\Psi_+$ ) in the void are shown.  $\sigma$  and  $\pi$  electrons of the graphite-layers are also shown.

simple model that the positrons are in a free state but effectively confined by the inner-most, namely void-wall, graphite layers of the voids. Since valence electrons of graphite are essentially of two dimensional, the electron state at the inner-most graphite layer is also nearly the same as that of graphite layer in the bulk. In this model the wave function of the positron is extended over the whole of the void. For small voids with diameter less than about 5 nm, the positron state will be given well by that of zero-point motion (ZPM). Therefore the void diameter, or an effective separation between the facing graphite void-wall layers (Fig.6(b)), determines positron annihilation lifetime and ACAR distribution. Hereafter we call this void-volume trapping to make distinction from conventional void-surface trapping in metals. Interaction between the void-wall and the volume-trapped positron will be subject of future study. However we note a volume effect stem from ZPM. Positrons confined in spherical infinite square-well potential with radius  $R_v$  will have the ZPM energy,  $E_0$ ,

$$E_0 = \frac{\pi^2 \pi^2}{2mR_v^2}$$

where  $m$  is the positron mass.  $E_0$  amounts to 1.5 eV for  $R_v=0.5$  nm and 0.48 eV for  $R_v = 1$  nm. This square-well potential might be too simple but could give us correct order of the ZPM energy. The smaller ZPM energy for the larger void is, at least one of, reason for the void volume-trapping.

Here we adopt an over-simplified picture that the positrons in the bulk graphite are confined in a void with diameter of the interlayer separation ( namely  $c/2$  ), neglecting an effect coming from difference of dimensionality of the confinement space : two dimensional for graphite bulk and three dimensional for voids.

One might suppose that positron emission from the void surface is energetically unfavorable, because positron work function of HOPG is reported to be about 1.5 eV [28,30]. It should be noted that this work function is for the emission along  $\langle 0001 \rangle$  direction from the basal-plane, and corresponds to energy barrier to be overcome by the positron when passing through the outermost graphite hexagonal network plane at the surface. However the positrons can move

layer space and are supposed to be emitted easily along the basal plane. Consequently if the void-wall contains the edge (such as zig-zag or arm-chair [17]) of graphite hexagonal networks, free positrons can be emitted there, perpendicular to  $\langle 0001 \rangle$ , to be confined in the voids.

For simplicity we assume the voids in glassy carbons are spherical in their shape, then the void radius,  $R_v$ , is related to  $R_g$ ,

$$R_v^2 = (5/3)R_g^2.$$

In Fig. 7 ACAR FWHM widths and lifetimes are plotted against the void radius calculated from the result of small angle neutron scattering shown in Tab.1, and further ACAR widths ( PZPC and PZNC ) and lifetime of HOPG are also shown for the effective separation of  $c/2$ . It is clearly seen that ACAR width decreases and lifetime increases with increase in the effective separation up to about 3 nm but are saturated for the further increase. This definitely demonstrates the overlapping between the positron wave function and the electron

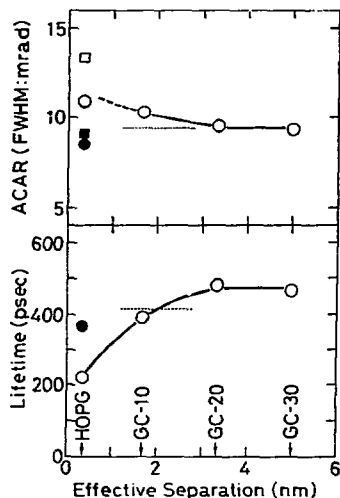


Fig.7. Relations between positron annihilation characteristics ( ACAR FWHM width and lifetime ) and the effective separation ( void diameter ). For ACAR width of HOPG, circles stand for PZNC and squares for PZPC orientation: open symbols are for unirradiated and solid ones are for irradiated HOPG-ZYH.

wave functions of the void-wall graphite. From Fig.7 we can make rough estimation of the void diameter from ACAR width or lifetime. The results about the irradiated HOPG-2YH are shown in Fig.7 by a closed square and circles at c/2 of the unirradiated state. These data indicate that the irradiation-induced defects are voids with the nearly the same diameter as those of GC-10 or GC-20, namely 20-30 nm. Because vacancy in graphite can migrate above 1000°C [31], these voids are not due to vacancy clustering but to microcracks produced by marked anisotropic change in the lattice constants: 10.2% dilatation in the c-axis whereas 0.7% shrinkage in the a-axis ( Tab.1 ). This marked anisotropy is due to carbon interstitial clusters, such as C<sub>2</sub> and C<sub>3</sub>, formed in the interlayer space, and is significant after irradiation at temperatures below 200°C [31].

We make a short remark about Ps formation in the voids. Free Ps emission is possible since positronium work function is negative ( -0.6eV ) [28]. Actually a narrow p-Ps peak with small intensity around the zero momentum portion of ACAR curve were found for HOPG [22] and Grafoil (from Union Carbide Co.) [32] which is an exfoliated recompressed sheet made from graphite particles: 0.35% and 2.5% of the p-Ps intensity for HOPG and Grafoil respectively. In present study, however, such a narrow p-Ps peak has not been detected.

### 3-3 C<sub>60</sub>/C<sub>70</sub> Fullerene

ACAR curve of the C<sub>60</sub>/C<sub>70</sub> powder agrees very well with that of GC-20 as shown in Fig.4. Lifetime spectrum of the powder is also similar to that of GC-20 ( Fig.4 ) and is represented by a single component of 417 psec which is in good agreement with the previous results by other groups [11-13]. It should be noted that these positron annihilation characteristics of C<sub>60</sub>/C<sub>70</sub> are completely the same as those observed for the glassy carbons and isotropic graphites. This indicates a positron trapping state in open volume which is very similar to the voids in glassy carbons.

The C<sub>60</sub> fullerene crystallite powder consists of the soccer ball molecules of 60-atom cage, which form FCC structure with a lattice constant of 1.42 nm [9](Fig.1). The soccer ball has a hollow-cage structure of truncated icosahedron which has a diameter of

0.71nm and consists of 12 pentagons and 20 hexagons [9,10]. In the cage bond lengths between C-C are 0.140 and 0.146 nm, which are very close to that in graphite hexagonal network (0.142 nm). This structure makes its electronic structure very similar to that in graphite, namely trigonal  $\sigma$  and  $\pi$  electrons. While within the cage the C-C bonding is very strong, the intermolecular ( C<sub>60</sub>-C<sub>60</sub> ) bonding is very weak and analogous to the interlayer bonding between graphite layers and also due to van der Waals attraction. Because of the weak intermolecular interaction, the solid C<sub>60</sub> has large open spaces, for example, at the octahedral interstices where potassium atoms can be accommodated in. The distance, van der Waals separation, between adjacent cages is about 0.29 nm, as compared with the interlayer distance ( 0.335 nm ) of graphite. Puska and Nieminen [14] calculated the positron wave function and lifetime within the local density approximation and suggested that the positron density is highly concentrated, but not delocalized, in the open volume of the octahedral interstices. They also calculated positron lifetime very similar to the experimental one. The nearly same calculations have been reported by Ishibashi et al. [15] and Jean et al. [12]. However, lifetime of about 400 psec has been commonly observed in glassy carbons as well as isotropic graphite and irradiated HOPG as shown above. The significant observation of present study is that the ACAR curve of C<sub>60</sub>/C<sub>70</sub> also agrees quite well with that of GC-20. In view of the fact that the ACAR curve and the lifetime of the C<sub>60</sub>/C<sub>70</sub> powder are very similar to those of the glassy carbons, positrons should be in the nearly the same state in both carbon materials. Further we have to note that C<sub>60</sub> has basically the same chemical bonding character as those in graphite and glassy carbon, namely trigonal sp<sup>2</sup> and  $\pi$ -electrons. Then we could reasonably assume that the positrons are trapped in open volume which size is given by the void volume-trapping model for the glassy carbons. The present results are shown by dashed lines in Fig.7 and indicates that positrons are trapped in open volume with diameter of about 2 nm, which is much larger than that at the octahedral interstices ( 0.71 nm ). To illustrate this a sphere of radius 2 nm centered on the soccer-ball lattice point is shown in Fig.8. The sphere is clearly found to be much bigger than an inscribed sphere at the octahedral interstice point, for



example  $O_T$ , and to have the nearly the same open volume as that estimated for the soccer-ball vacancy where one molecule of  $C_{60}$  is missing. This strongly suggests the positron trapping at the soccer-ball vacancy with ample trapping rate from the delocalized state.

We consider possibility of positron trapping in inter-granular open space of the powder: grain size of the powder is order of  $10^{-7}$  m. If positrons are trapped there, their lifetime will show no change upon cooling. Positron lifetime, however, was found to decrease slightly with temperature down to 10K: about 10 psec shorter at 10K than that at room temperature, as shown in Tab.1. This is due to the small reduction of the open volume caused by lattice shrinkage at low temperature: shrinkage in  $a_0$  at 11 K is about 1% [33]. This reduction can be evidence of the volume-trapping of nanometer-scale rather than of micron-scale for the inter-granular open space.

In this context, we note that nearly the same reduction has been also predicted theoretically for the delocalized positrons by Puska and Nieminen. In their model the positrons are concentrated in the octahedral interstices. Then it should be pointed out that positron lifetime is sensitive to the lattice parameter and that positrons in

$C_{60}$  are localized or nearly localized in open volume but not the void surfaces or soccer-ball surface.

In summary, we have done systematic study of various kind of carbon materials, HOPG, isotropic fine-grained graphite, glassy carbon and  $C_{60}/C_{70}$  powder, and have found similar ACAR curves and lifetimes common to them. These are come from the void-volume trapping and experimentally correlated to the void size obtained from small angle neutron scattering. Based on the correlation the positron-trapping open volume is roughly estimated about 2 nm in diameter and shown to correspond to the volume around the soccer ball vacancy. This strongly suggests existence of the soccer-ball vacancy in  $C_{60}/C_{70}$  crystallite.

We thank staff members of the Oarai Branch of IMR, Tohoku University for their help in handling irradiated samples and positron sources.

#### REFERENCES

- (1) Brandt, W. and Dupasquier, A.(Ed.): "Positron Solid-State Physics" (North-Holland, Amsterdam, 1983).
- (2) Aravin, L.G., Salukvadze, R.A., Shantarovich, V.P. and Khomenko, A.A.: phys. stat. sol.(a) 50, K213 (1978).
- (3) Iwata, T., Fukushima, H., Shimotomai, M. and Doyama, M.: Jp. J. Appl. Phys., 20, 1799 (1981).
- (4) Shimotomai, M., Iwata, T., Takahashi, T. and Doyama, M.: J. Phys. Soc. Japan, 52, 694 (1983).
- (5) Kuramoto, E., Takenaka, M., Hasegawa, M. and Tanabe, T.: J. Nucl. Mat., 179-181, 202 (1991).
- (6) Hasegawa, M., Kajino, M., Kueahara, H., Kuramoto, E., Takenaka, M. and Yamaguchi, S.: Mater. Sci. Forum, 105-110, 1041 (1992).
- (7) Kratschmer, W., Lamb, L.D., Fostiropoulos, K. and Huffman, R.: Nature, 347, 354 (1990).
- (8) Hebard, A.F., Rosseinsky, M.J., Haddon, R.C., Murphy, D.W., Glarum, S.H., Palstra, T.T.M., Ramirez, A.P. and Kortan, A.R.: Nature, 350, 600 (1991).

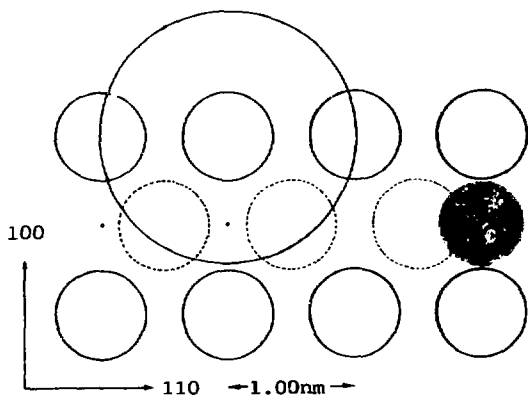


Fig.8. The soccer-ball array in the (110) plane and possible open volume in  $C_{60}$ . Dashed circles represent the soccer ball on the neighboring (110) plane. Octahedral interstice is shown by a circle with mesh ( $O_T$ ). Large circle represents a sphere with diameter of 2 nm : approximating size of the soccer-ball vacancy.

- (9) Huffman, D.R.: *Phys. Today*, 44, 22 (1991).
- (10) Prassides, K. and Kroto, H.: *Phys. World*, 5, 14 (1992).
- (11) Azuma, T., Saito, H., Yamazaki, Y., Komaki, K., Nagashima, Y., Watanabe, H., Hyodo, T., Kataura, H. and Kobayashi, N.: *J. Phys. Soc. Japan*, 60, 2812 (1991).
- (12) Jean, Y.C., Lu, X., Lou, Y., Bhanthi, A., Sunder, S.C., Lyu, Y., Hor, P.H. and Chu, C.W.: *Phys. Rev.*, 45, 12126 (1992).
- (13) Schaefer, H.E., Forster, M., Wurschum, R., Kratschmer, W. and Huffman, D.R.: *Phys. Rev.*, 45, 12164 (1992).
- (14) Puska, M.J. and Nieminen, R.M.: *J. Phys.: Condens. Matter*, 4, L149 (1992).
- (15) Ishibashi, S., Terada, N., Tokumoto, M., Kinoshita, N. and Ihara, H.: *ibid*, 4, L169 (1992).
- (16) Engle, G.B.: *Carbon*, 8, 485 (1970).
- (17) Marsh, H.(Ed.): "Introduction to Carbon Science". (Butterworths, London, 1989).
- (18) Shiraishi, M.: "Introduction to Carbon Materials" (in Japanese), Ed. by Inagaki, M., (Carbon Materials Soc., Tokyo, 1984), p29.
- (19) Aizawa, K., Yamaguchi, S., Niimura, N. and Hasegawa, M.: *Sci. Rep. RITU (Tohoku Univ.)*, 35, 189 (1991).
- (20) Berko, S., Kelley, R.E. and Plaskett, J.S.: *Phys. Rev.*, 106, 824 (1957).
- (21) Colombino, P., Fiscella, B. and Trossi, L.: *Nuovo Cimento*, 27, 589 (1963).
- (22) Lee, R.R., von Stetten, E. C., Hasegawa, M. and Berko, S.: *Phys. Rev. Lett.*, 58, 2363 (1987).
- (23) Yongming, L., Johansson, B. and Nieminen, R.M.: *J. Phys.: Condens. Matter*, 3, 2057 (1991).
- (24) Schultz, P.J. and Lynn, K.G.: *Rev. Mod. Phys.*, 60, 701 (1988).
- (25) Rothwell, W.S.: *J. Appl. Phys.*, 39, 1840 (1968).
- (26) Hasegawa, M., Yoshinari, O., Matui, H. and Yamaguchi, S.: *J. Phys. Condens. Matter*, 1, SA77 (1989).
- (27) Jensen, K.O., Eldrup, M., Singh, B.N., Linderoth, S. and Benzon, M.D.: *J. Phys. F. Met. Phys.*, 18, 1091 (1988).
- (28) Sferlazzo, P., Berko, S., Lynn, K.G., Mills, Jr., A.P., Roellig, L.O., Viescas, A.J. and West, R. N.: *Phys. Rev. Lett.*, 60, 538 (1988).
- (29) Saito, R., Shima, N. and Kamimura, H.: *Synthetic Metals*, 23, 217 (1988).
- (30) Gullikson, E.M. and Mills, Jr., A.P.: *Phys. Rev.*, B36, 8777 (1987).
- (31) Kelly, B.T.: "Physics of Graphite" (Applied Science Pub., London, 1981).
- (32) Hasegawa, M., Kajino, M. and Yamaguchi, S.: To be published.
- (33) Heiney, P.A., Fischer, J.E., McGhie, A.W., Romanow, W.J., Denenstein, A.M., McCauley, Jr., J.P., Smith, III, A.B. and Cox, D.E.: *Phys. Rev. Lett.* 66, 2911 (1991).